# Theoretical Study of Endohedral $C_{36}$ and Its Dimers

**Hong Seok Kang***

*College of Liberal Arts, Jeonju University, Hyoja-dong, Wansan-ku, Chonju, Chonbuk 560-759, Republic of Korea*

*Received: October 13, 2005; In Final Form: February 14, 2006*

It is found that atoms of lithium and carbon can be encapsulated in $C_{36}$ on the basis of the calculation of their encapsulation energies using density functional theory. Specifically, they can be encapsulated in $C_{36}$ better than in $C_{60}$ despite the smaller (70%) cavity size of the former. In $C@C_{36}$, the encapsulated carbon atom forms covalent bonds with the carbon atoms of the cage, which is in contrast with the case of $N@C_{60}$. Two isomers are expected to be in an equilibrium which involves spin quenching and generation. $Li@C_{36}$ and $C@C_{36}$ are expected to exist in the form of dimers with nonendohedral fullerenes, i.e., as $Li@C_{36}-C_{36}$ and $C@C_{36}-C_{36}$. Three stable isomers were found for the former (A, B, and C). Equilibrium between A and C as well as that between B and C is accompanied by spin transfer between two fullerene units, while that between A and B is not. The two stable isomers in $C@C_{36}-C_{36}$ form an equilibrium accompanied by spin quenching and generation, allowing the dimer to be potentially useful for molecular devices.

## Introduction

Since the discovery of fullerene, various kinds of endohedral fullerenes have been prepared.[1,2] Many of them are stable under ambient conditions even though empty cages have never been isolated in some cases. Electronic and chemical properties of fullerenes can be modified upon atom encapsulation. Particularly, charge transfer and ionic interaction play a crucial role in manipulating the properties of metallofullerenes.[3] Recently, much attention has been paid to the study of metallofullerene, in which the encasement extends to a group of atoms involving transition metals.[4] In addition, the encapsulation of metallofullerene molecules in nanotubes has been reported.[5] It has also been shown that the metallofullerenes are promising candidates for electronic, optical, and biomedical applications.[6]

Encapsulation of nonmetallic atoms works through a mechanism that is entirely different from that of metal atoms in that no appreciable charge transfer is involved. For example, the $C_{60}$ cage works as a chemical Faraday cage, in which very reactive paramagnetic atoms such as nitrogen and phosphorus retain their atomic characters after they are encased.[7] Furthermore, no covalent interactions exist between those atoms and the fullerene cage. The comparison of $N@C_{60}$ and $N@C_{70}$ shows that the difference in the shape of the host cage affects the charge and spin density distributions of the encased nitrogen atom.[8] It is reasonable to conclude that energetic bombardment of ions,[7] which is usually used for the nitrogen encapsulation, is able to house nonmetallic atoms other than nitrogen. In this respect, this study investigates such a possibility for a carbon atom, focusing on the question of whether the carbon atom also retains its atomic character after encasement or can make covalent bonds to the cage.

Piskoti et al. recently introduced a method to synthesize $C_{36}$ using the arc-discharge method, which is the first fullerene smaller than $C_{60}$ synthesized in bulk amount.[9] Their nuclear magnetic resonance measurement indicates $D_{6h}$ symmetry of the molecule. Theoretical calculation shows that there can exist another isomer with $D_{2d}$ structure which is nearly isoenergetic to the $D_{6h}$ structure.[10] Violation of the isolated pentagon rule indicates the high reactivity of the molecule. In agreement with this, measurement of its electronic spectra suggests that the molecule may exist in the form of dimers and trimers rather than monomers.[11] As a matter of fact, dimerization of the molecule was shown to occur without an activation barrier.[12] The fullerene is particularly interesting, since a strong electron−phonon coupling in the molecule opens the possibility of using it for a superconductor with a transition temperature even higher than that of alkali-metal-doped $C_{60}$ solids.[13]

Much more interesting applications can be found if an endohedral $C_{36}$ can be synthesized, since it can reveal novel electronic and magnetic properties not observed in a nonendohedral fullerene, especially because it prefers to form dimers and polymers. Although the cavity size of the molecule is smaller than that of $C_{60}$, it can still encapsulate a small atom. [The shorter diameter of the molecule is still ∼5 Å long.] In fact, $U@C_{36}$ was identified from a laser vaporization experiment with graphite.[14] Inspired by this finding, preliminary calculations were done for $M@C_{36}$ (M = Li, Na, and K),[15] $He@C_{36}$,[16] and $N@C_{36}$.[16] Herein I describe a detailed investigation on the possible encapsulation of lithium, carbon, and nitrogen using density functional theory. To elucidate the effect of a small size of the fullerene cage, comparison will be also made to the corresponding encasement in $C_{60}$. If the encasement is shown to be plausible, the possibility of dimer formation will also be investigated. In doing this, stable isomers will be searched for the dimers $X@C_{36}-C_{36}$ (X = Li and C), which can be produced when the corresponding endohedral fullerenes are diluted by empty fullerenes. Particular attention will be paid to the possible spin transfer from the encasing unit to the other as well as to the possible spin generation and quenching among various isomers in the equilibrium, since it may have applications in molecular electronics,[17] memory devices,[18] and information storage.[19]

* E-mail: hsk@jj.ac.kr.

10.1021/jp055850l CCC: $33.50 
Published on Web 03/22/2006

## Theoretical Method

The total energy calculations are performed using the Vienna ab initio simulation package (VASP).[20] Electron−ion interaction is described by the projected augmented wave (PAW) method,[21] which is equivalent to a frozen-core all-electron calculation. The exchange-correlation effect is treated within the generalized gradient approximation presented by Perdew, Burke, and Ernzerhof (PBE).[22] Solution of the Kohn−Sham (KS) equation is obtained using the Davison blocked iteration scheme followed by the residual vector minimization method. All valence electrons of chemical elements are explicitly considered in the KS equation. I adopt a supercell geometry in which *k*-space sampling is done with the Γ-point, using large supercells which guarantee interatomic distances between neighboring cells greater than 7.00 Å. The cutoff energy is set high (400 eV) enough to guarantee accurate results, and the conjugate gradient method is employed to optimize the geometry until the Hellmann−Feynman force exerted on an atom is less than 0.03 eV/Å. All the results rely on the spin-polarized calculation. The reliability of the PBE calculation within the PAW was confirmed in the recent calculations on the electronic and chemical properties of metal−aromatic sandwich complexes.[23]

## Results

First, I report my calculation on Li@$C_{36}$ very briefly. The structure of the $C_{36}$ molecule is assumed to have $D_{6h}$ symmetry throughout this work, as was suggested by a nuclear magnetic resonance measurement.[9] The calculation of the encapsulation energy (−2.06 eV) strongly indicates that a lithium atom can be encased in $C_{36}$. The atom is displaced from the center of the cage by 0.51 Å along the long axis passing through the center of the cage. Therefore, there are two equivalent sites for the atom on the axis. However, the barrier (0.03 eV) between the two sites is very small, and thus, the Li atom can move freely at least by 1.02 Å (= 0.52 × 2) between the sites. The encapsulation energy shows that it is more favorable to encapsulate the atom in $C_{36}$ than in $C_{60}$, noting that the encapsulation energy in the latter fullerene is −1.33 eV. My analysis shows that there is a large charge transfer from Li to the cage as well as a complete spin transfer, resulting in the large electrostatic stabilization between $Li^+$ and $C_{36}^-$. Consistent with this, the natural bond orbital (NBO) analysis[24] with PBEPBE/6-31G(d) using the GAUSSIAN03[25] program shows that the charge on the Li atom is 0.69.

Next, I mention the possible encapsulation of a nitrogen atom in $C_{36}$. I have optimized the geometry starting from three different initial positions of the nitrogen atom in the cage, and my description will be focused on the structure which gives the lowest energy among the three. The energy of nitrogen encapsulation $E_{en}$ (+0.20 eV), calculated from the energy change of the process $C_{36} + N \rightarrow N@C_{36}$, is slightly larger than that (+0.03 eV) of the corresponding process involving $C_{60}$, suggesting the possible existence of N@$C_{36}$ as a metastable complex. This may reflect the size of the $C_{36}$ cage, which is smaller than that of $C_{60}$. As shown in Figure 1, the nitrogen atom is displaced from the center of the fullerene cage ($C_s$ symmetry), forming $sp^3$ bonds with three carbon atoms (C15, C16, and C22). This is clearly different from Slanina and Chow's result that showed that the nitrogen atom was located in the central position.[16] I also find a local minimum at the same position, although the configuration is less stable by 1.00 eV than the one shown in Figure 1. In the figure, bond lengths to the three carbon atoms are 1.49, 1.52, and 1.52 Å, respectively. The ground-state spin configuration is a doublet, which is different from that (quartet) of N@$C_{60}$. In addition, my separate analysis shows that the nitrogen atom does not hold any appreciable amount of spin density, implying that all the spin density was transferred to the fullerene cage. This is also different from the case of N@$C_{60}$, in which the nitrogen atom is located at the center of the cage with no appreciable amount of spin transfer.

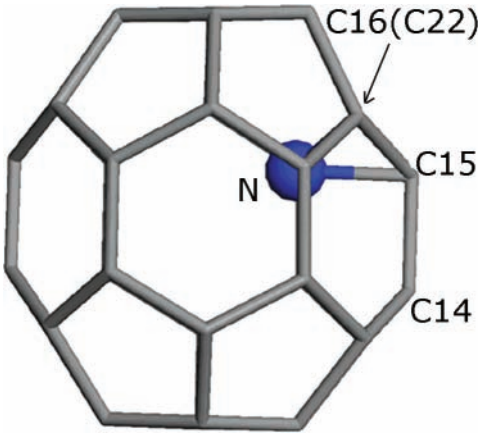


**Figure 1.** Optimized structure of N@$C_{36}$.

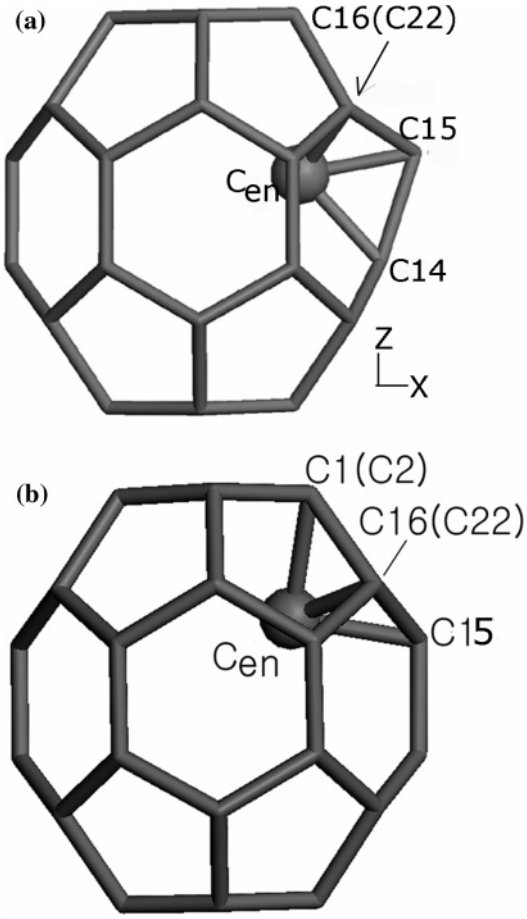


**Figure 2.** Optimized structures of two stable isomers, A (a) and B (b), of C@$C_{36}$.

It will also be interesting to see if an encasement of carbon can be achieved. The first step for this is to calculate the energy of carbon encapsulation in $C_{36}$. I find two nonequivalent sites, each of which corresponding to isomers A (triplet) and B (triplet) shown in Figure 2. Their energies are different from each other only by 0.11 eV. [The center of the cage is not a site corresponding to a local minimum, which is different from

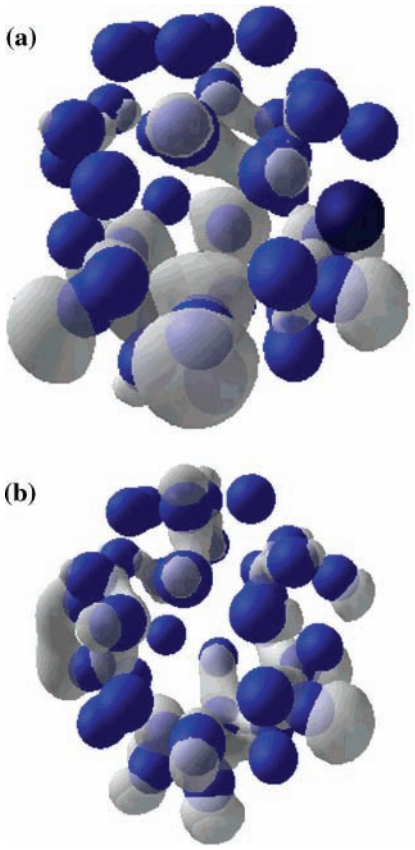


**Figure 3.** Electron density distributions in the SOMO − 1 (a) and SOMO (b) for isomer A of $C@C_{36}$.

the case of $N@C_{60}$.] For isomer A, which is more stable than the other, a large negative value (−1.92 eV) of $E_{en}$ surprisingly shows that a carbon atom ($C_{en}$) can be encapsulated in $C_{36}$ much more favorably than a nitrogen atom ($E_{en} = +0.20$ eV). The energy is even comparable to the encapsulation energy (−2.06 eV) of Li in $C_{36}$. In addition, it is even larger than the encapsulation energy of a nitrogen atom in $C_{60}$ (+0.03 eV), leading to the conclusion that indeed experimental work would be able to identify $C@C_{36}$. [$N@C_{60}$ was experimentally identified.] Figure 2 shows that the optimized structure is similar to that of $N@C_{36}$. $C_{en}$ is significantly displaced from the center of the fullerene cage toward the inner wall of the cage ($C_s$ symmetry). $C_{en}$ is almost neutral, as shown by its NBO charge (−0.06). The atom is bonded to four carbon atoms (C14, C15, C16, and C22) of the fullerene cage with bond lengths of 1.57, 1.55, 1.56, and 1.56 Å, respectively. Compared to $N@C_{36}$, there is one more bond, $C_{en}$−C14. My separate analysis of the NBO shows that the Wiberg bond indices (WBIs)[26] are 0.76, 0.70, 0.78, and 0.78. Another structural feature is that C15 protrudes from the surface of the fullerene cage by approximately 1.47 Å, manifesting its $sp^3$ character. Bonds C14−C15, C15−C16, and C15−C22 are weakened to single bonds as shown by the increased bond lengths (1.55, 1.56, and 1.56 Å, respectively) compared to those (1.43, 1.44, and 1.44 Å) in the free $C_{36}$. All these observations suggest that there should remain no appreciable amount of spin density around $C_{en}$. As in the case of $N@C_{36}$, we can observe a complete spin transfer from $C_{en}$ to the fullerene cage upon encasement. Figure 3 shows that one of the two unpaired electrons is concentrated on six carbon atoms located at the lower part of the cage, while the other one is distributed over the whole cage, each of them filling spin-up states (not spin-down states) of the SOMO − 1 and SOMO (singly occupied molecular orbital), respectively. The net spin

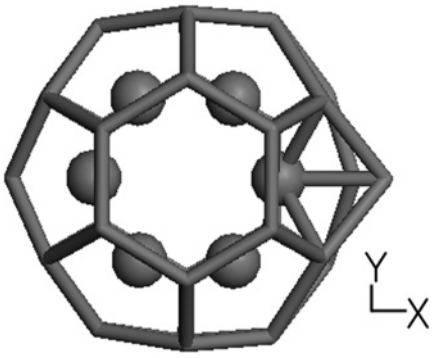


**Figure 4.** Six equivalent sites of $C_{en}$ in the cavity of $C_{36}$ viewed along the *z*-axis for $C@C_{36}-C_{36}$.

density is mainly concentrated on atoms around the south pole along the *z*-axis. A separate analysis shows that this electronic structure can be understood if an electron is removed from the spin-paired HOMO orbital of $N@C_{36}$ (doublet) in an imaginary process of replacing the encased nitrogen atom by a carbon atom. [The HOMO of $N@C_{36}$ is equivalent to the SOMO of $C@C_{36}$, and the SOMO of the former to the SOMO − 1 of the latter. Here, I label the top of the spin-paired level HOMO, and spin-unpaired levels SOMO − 1 and SOMO, etc.]

In isomer B, $C_{en}$ is also neutral, as manifested by its NBO charge (0.02). Compared to isomer A, there is one more (five) C−C bond involving the atom $C_{en}$. The bonds comprise $\eta^5$-hapticity from $C_{en}$ to the carbon atoms (C1, C2, C22, C15, and C16 in Figure 2b) of a five-membered ring. Individual bonds involving $C_{en}$ are weaker, as shown by their WBIs (0.42, 0.42, 0.57, 0.52, and 0.57), which are smaller than those in isomer A. Consistent with this, their bond lengths (1.76, 1.76, 1.64, 1.65, and 1.64 Å) are longer than those in isomer A, particularly for $C_{en}$−C1 and $C_{en}$−C2 bonds. Contrary to the case of isomer A, the C1−C16 and C15−C16 lengths are almost the same as in the fullerene without $C_{en}$ encapsulated. An analysis shows that the spin density distribution is similar to that of isomer A in that it is more or less concentrated around the south pole.

The $D_{6h}$ symmetry of the fullerene and the geometry of $C_{36}$ explained above lead us to expect 24 cavity sites where $C_{en}$ can be located in $C@C_{36}$. Half (set A) of them correspond to isomer A, and the remaining half (set B) to isomer B. Again, half of set A has $C_{en}$ on the lower half of the cavity along the *z*-axis, and the remaining half has $C_{en}$ on the upper half in Figure 2. [See Figure 2 for the definition of the coordinate system. In the figure, $C_{en}$ is shown to be located on the upper half of the cage.] A similar argument holds for set B. Figure 4 also shows six equivalent sites on one half viewed along the *z*-axis. One can propose that those 24 sites represent different states of a memory storage device, for which it is desirable that all of them are accessible from one another at room temperature. The calculation of the energy of intermediate states shows that six equivalent sites, related to one another by $C_6^n$ ($n = 1, 6$) rotations along the *z*-axis, are separated by one another by energy barriers of heights 0.71 and 0.51 eV for sets A and B, respectively, while the sites of set A equivalent to one another by the reflection in $\sigma[xy]$ are separated by a barrier of height 0.52 eV. The barrier for the conversion from isomer B to isomer A is ∼0.15 eV. Therefore, the encapsulated carbon atom should be able to jump from one designated location to another at a reasonable rate at room temperature.

For comparison, I also have considered the encapsulation of carbon in $C_{60}$. There are two stable isomers (isomers A and B) similar to isomers A and B of $C@C_{36}$. Similarly to the case of the latter, isomer A is 0.20 eV more stable than isomer B. The

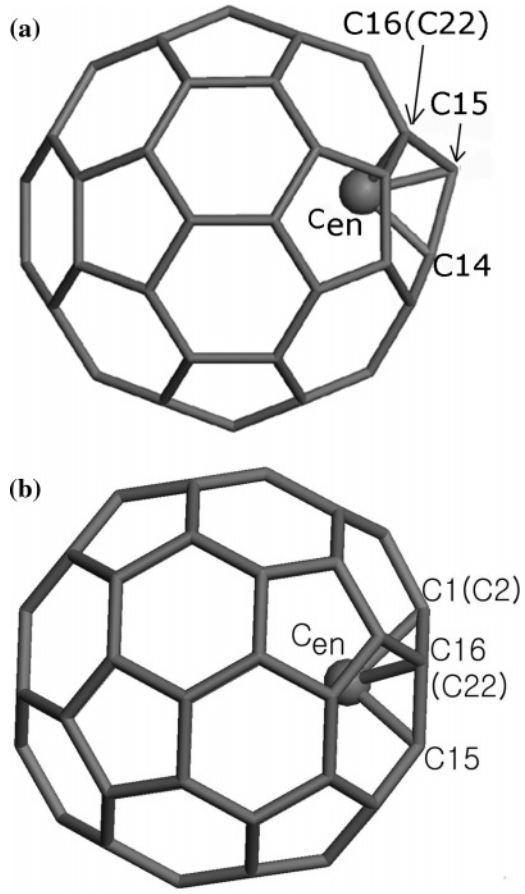


**Figure 5.** Optimized structures of isomers A (a) and B (b) of $C@C_{60}$.

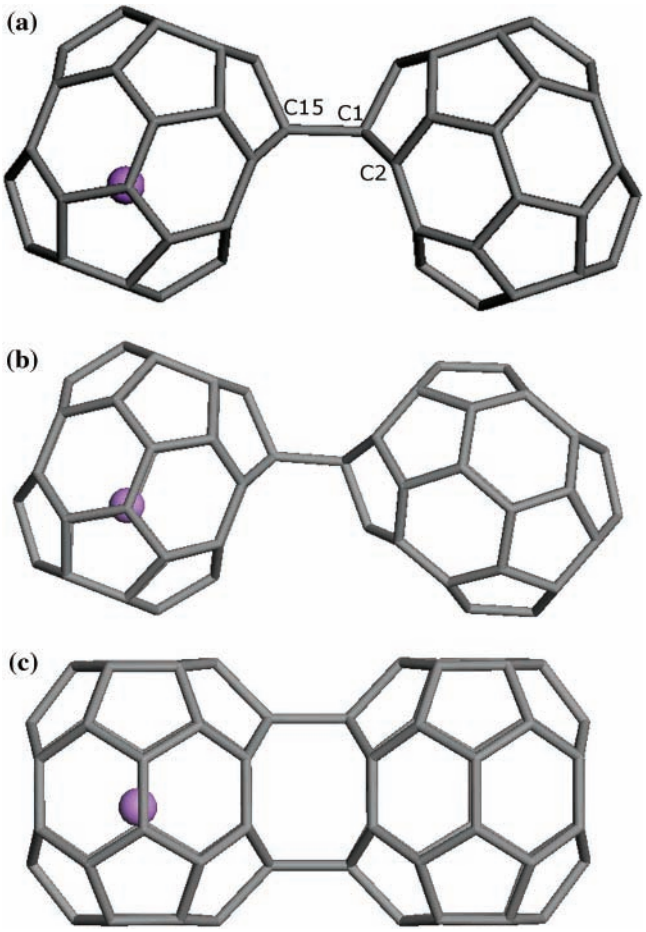


**Figure 6.** Optimized structures of three isomers, A (a), B (b), and C (c), of the dimer $Li@C_{36}-C_{36}$.

calculation shows that the encapsulation is energetically less favorable ($E_{en} = -1.35$ eV for isomer A) than that in $C_{36}$, reflecting the lower chemical reactivity of $C_{60}$ inside the cage. Figure 5 shows that $C_{en}$ is also displaced from the center of the cage and is bonded to four or five carbon atoms in a way very similar to that in the case of $C@C_{36}$. For simplicity, I label the carbon atoms so that equivalent atoms have the same labels in the two systems. In isomer A, there are 60 equivalent sites of $C_{en}$, since it is located on top of a carbon atom of the fullerene. C15 also protrudes from the surface of the cage by 1.57 Å, and interatomic distances from $C_{en}$ to C14, C15, C16, and C22 are 1.58, 1.57, 1.66, and 1.66 Å, respectively. Therefore, the $C_{en}-$C16 and $C_{en}-$C22 distances are 0.10 Å longer than those in the case of $C@C_{36}$, which is also manifested in the bond orders (0.64) being smaller than the corresponding ones in $C@C_{36}$. The bond length (1.48 Å) between C14 and C15 is only slightly elongated from that (1.45 Å) in the unencapsulated $C_{60}$. The spin configuration (singlet) is different from that (triplet) of $C@C_{36}$, even though there is a striking similarity in the structures of the two systems around C15. [The conformation (triplet) which has $C_{en}$ at the center of the cage, although it corresponds to a local minimum, is found to be much less stable ($E_{en} = -0.03$ eV).]

In isomer B, little deformation is involved in the geometry of the fullerene cage. Bond lengths for all five bonds involving $C_{en}$ (1.75 Å) are the same, indicating perfect $\eta^5$-hapticity. There are 12 equivalent sites of $C_{en}$ in this isomer, since there are 12 pentagons in $C_{60}$. The spin configuration (triplet) is different from that of isomer A, showing its sensitivity to the position of $C_{en}$. Since the relative energy of isomer B is only 0.20 eV higher than that of isomer A, the two isomers will be in an equilibrium that involves spin quenching and generation. More precisely, there is an equilibrium among 72 distinct sites, i.e., 60 sites of isomer A and 12 sites of isomer B. This shows the possible application in magnetic devices or spin-based electronics, since the two sets of sites can be distinguished from each other by the difference in spin or magnetic properties. The locations of the carbon atom in Figure 5 are in clear contrast to those in the case of $N@C_{60}$ for which the nitrogen atom is located at the center of the cage. This shows that the structure of an endohedral fullerene is critically dependent upon the kind of encased atom.

Next, the dimerization of $Li@C_{36}$ will be taken into account through the reaction $Li@C_{36}(1) + C_{36}(2) \rightarrow Li@C_{36}(1)-$C36(2). [I put the labels "1" and "2" in parentheses to distinguish the two fullerene units.] The dimerization can be considered to be plausible, noting that it was proposed that a covalently bonded dimer can be a dominant structural unit in the nonendohedral $C_{36}$ thin films.[11] Investigation of the heterodimer would be particularly interesting, since the majority of the product will still be metal-free even after the treatment for metal encapsulation. For the structure optimization, four different isomers were considered where bonding between the two cages occurs at different carbon atoms. Optimized structures for three of them (A, B, and C) are shown in Figure 6. [The spin configuration is a doublet for all the isomers.] Another isomer, which retains no bonding between the two cages after optimization, can be generated if unit 1 is bonded to carbon atom C2 of unit 2 instead of C1 in Figure 6a. Among the three possible isomers shown in the figure, isomers A and B are characterized by single bonds between two units at different carbon atoms, while there are two single bonds in isomer C. I find only one

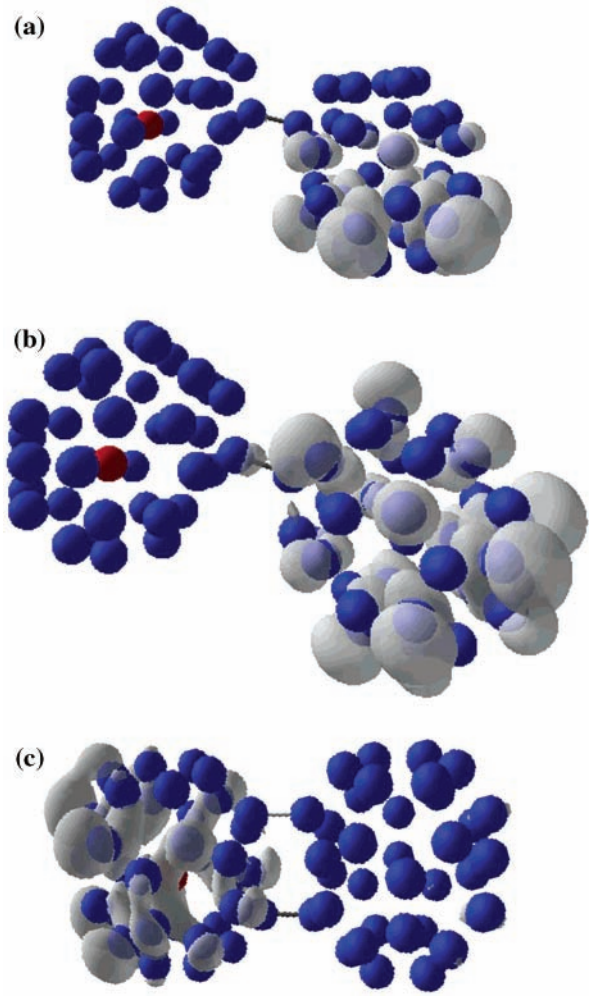


**Figure 7.** Spin density distributions of three isomers, A (a), B (b), and C (c), of the dimer Li@$C_{36}$−$C_{36}$ shown in Figure 6.

stable site of Li for each of the isomers A and B, which is shown in Figure 6. This is because the symmetry of the potential energy surface inside the cavity is broken upon the formation of the dimer. For example, a possible location of Li in the upper half cavity in unit 1 is not energetically stable for isomers A and B. Although the symmetry of isomer C indicates that there are two equivalent locations (one on the upper half and the other on the lower half) of Li, the potential energy surface, which is nearly flat within 0.01 eV between the two sites, leads us to consider them as one site. In short, there is effectively only one possible site for Li in each of the three isomers. It is found that the dimerization energies (−1.50, −1.13, and −1.46 eV, respectively) of the three isomers A−C are comparable to one another. Therefore, the dimerized products would be a mixture of all three isomers. In the process of dimerization forming isomers A and B from their monomeric components, there is almost a complete transfer of spin from unit 1 to the other unit, while the spin density remains on unit 1 in isomer C. [See Figure 7.] Therefore, equilibrium between isomers A and C as well as that between B and C is accompanied by spin transfer between the two fullerene units, which does not happen between A and B.

It would also be quite valuable to investigate the dimerization of C@$C_{36}$ with a nonendohedral $C_{36}$ through the reaction C@$C_{36}$(1) + $C_{36}$(2) → C@$C_{36}$(1)−$C_{36}$(2). In doing this, I have considered four different isomers of the dimer where bonding between the two cages occurs at different carbon atoms. The optimized structures of three of them (A, B, and C) are shown

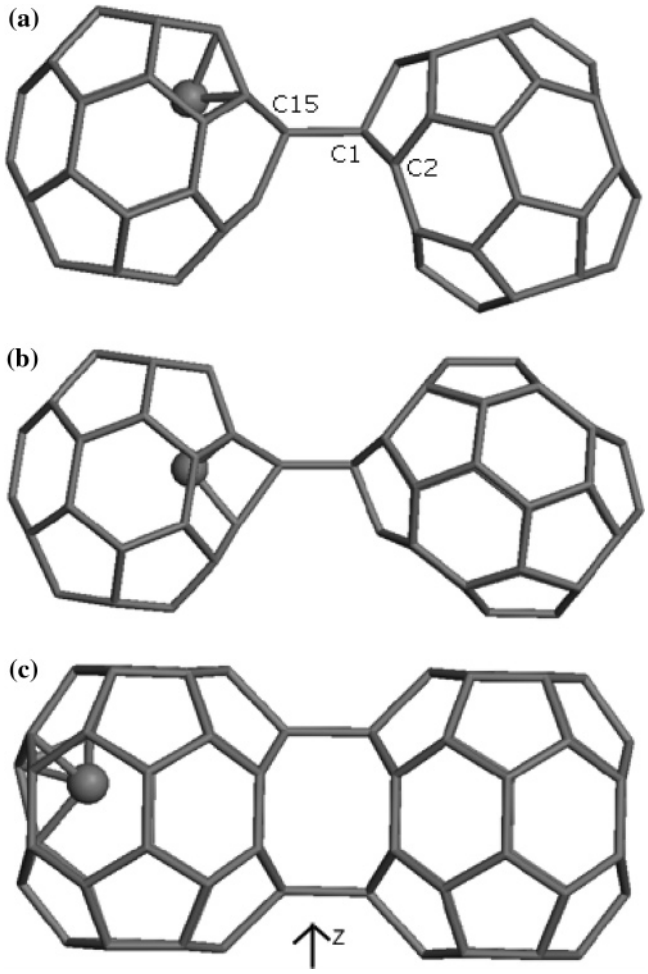


**Figure 8.** Optimized structures of three isomers, A (a), B (b), and C (c), of the dimer C@$C_{36}$−$C_{36}$.

in Figure 8. Another isomer, which retains no bonding between the two cages after optimization, can also be generated if unit 1 is bonded to carbon atom C2 of unit 2 instead of C1 in Figure 8a. Isomer C (singlet) is the most stable, in which two single bonds (bond lengths 1.62 Å) are formed between carbon atoms of the two units. There are four C−C single bonds involving $C_{en}$ with bond lengths of 1.55, 1.57, 1.57, and 1.57 Å. [In agreement with an earlier report,[11] the calculation shows that a similar structure is the most stable among all the dimerized isomers of $C_{36}$(1)−$C_{36}$(2) without a carbon atom encapsulated.] It is more stable than the optimized structure of isomer A by 0.28 eV, and then isomer B by 1.61 eV. For isomer C, the large negative energy of dimerization (−1.56 eV) indicates that C@$C_{36}$ would presumably exist in the form of dimers or polymers once it is formed.

In isomer A (triplet), there is a single bond between carbon atoms [C15(1) and C1(2)] of the two units with a bond length of 1.56 Å. This kind of bond formation is quite natural, since C15(1) protrudes from the surface of the cage in an isolated C@$C_{36}$. It is only slightly (0.28 eV) less stable than isomer C. $C_{en}$ is located at a position similar to that in isomer B of the monomer C@$C_{36}$ shown in Figure 2b. In fact, the isomer is much more stable than isomer B, which has $C_{en}$ at the same position as in isomer A of the monomer. The appreciable value of the dimerization energy (−1.28 eV) of isomer A indicates the possibility of its coexistence with isomer C. [The isomer of $C_{36}$(1)−$C_{36}$(2), i.e., that similar to isomer A shown in Figure 8a without a carbon atom encapsulated, has a very weak bonding between the two cages, as manifested by a small (−0.23 eV)

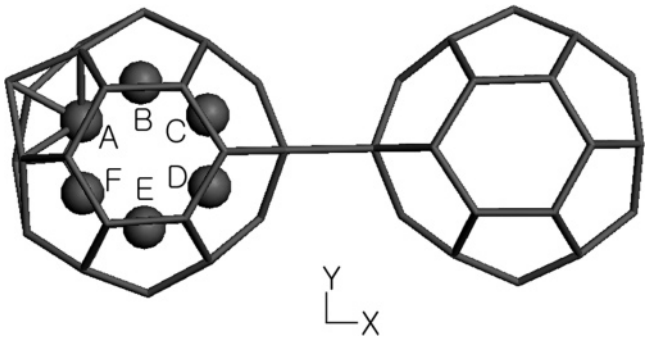


**Figure 9.** Possible sites of $C_{en}$ in the cavity of $C_{36}$ viewed along the *z*-axis for $C@C_{36}-C_{36}$. Sites A, B, and C are equivalent to sites F, E, and D by molecular symmetry.

energy of dimerization. Namely, the stabilization of isomer A is closely related to the carbon encapsulation.]

For isomer C, a lengthy calculation shows that there are twenty-two discrete locations for $C_{en}$, i.e., two less sites than those in the monomer $C@C_{36}$. To find this, I have optimized structures starting from six nonequivalent initial positions of $C_{en}$ similar to those in $C@C_{36}$, three (A, B, and C) of which, corresponding to the sites in isomer A of the monomer $C@C_{36}$, are shown in Figure 9. The other three are located at sites similar to those in isomer B of the monomer. [See Figure 8c for the definition of the *z*-axis.] Among all the sites, the one shown in Figure 8c corresponds to the one with the lowest energy. Relative energy values of all sites are within 0.00−0.47 eV with singlet spin configurations. Therefore, a nonnegligible degree of differentiation is introduced into the energy levels of the sites as a result of the dimer formation. Again, barriers separating those designated locations can be surmounted at room temperature because barrier heights are found to be 0.81 eV at most. In isomer A of the dimer, it is also found that there are 22 distinguished sites of $C_{en}$, and the most stable one is shown in Figure 8a. Relative energy values (eV) of the sites lie within 0.79 eV of each another. A lengthy calculation shows that the barriers for interconversion among all the sites are less than 0.57 eV. In summary, interconversion between isomers A and C does not change the total number of distinct sites for $C_{en}$, and those sites are accessible from one another at room temperature.

Although the spin configuration (triplet) of isomer A of $C@C_{36}(1)-C_{36}(2)$ is the same as that in an isolated $C@C_{36}$, an analysis shows that the spin density does not exclusively reside on $C@C_{36}(1)$. Figure 10 shows the electron density distributions in the SOMO − 1 and SOMO of the dimer, each of which is half-filled for spin-up states only. In the SOMO − 1, electron density is exclusively concentrated on the second unit $C_{36}(2)$, while the density resides exclusively on $C_{36}(1)$ in the SOMO. In summary, half of the total spin density is expected to be transferred from $C_{36}(1)$ to $C_{36}(2)$ upon the formation of isomer A from its components. Since there is no spin polarization in isomer C, isomerization between isomers A and C is accompanied by spin quenching and spin generation. [It is not necessary to consider isomer B, since it is energetically much less stable.] Since the C−C bonds between the two fullerene units involve different carbon atoms in the two isomers, isomerization between them should go through the breaking and formation of appropriate C−C bonds. In other words, the transition state for the interconversion should be the system of two isolated fullerene units. Therefore, the activation barrier of the conversion of A → C is approximately 1.28 eV, which is the dimerization energy of isomer A, and that of the reverse process is ∼1.56 eV. At low temperatures, isomer C should dominate the dimer, and the relative amount of isomer A should increase as the temperature increases. Therefore, this would apparently lead to the spin crossover from a low-spin state of isomer C to a high-spin state of isomer A at a certain temperature, resulting in the characteristic magnetothermal response of the system.

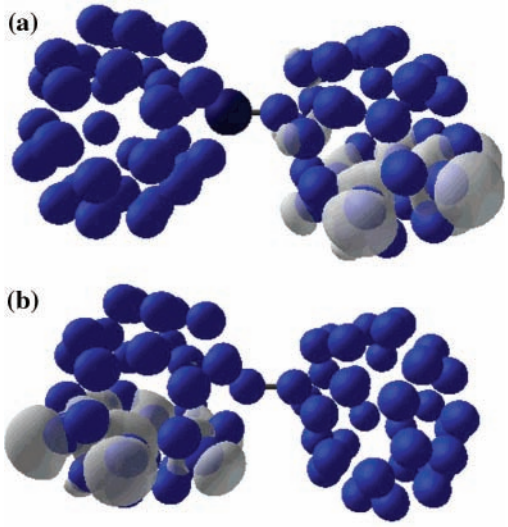


**Figure 10.** Electron density distributions in the SOMO − 1 (a) and SOMO (b) of isomer A of the dimer $C@C_{36}-C_{36}$ shown in Figure 8a.

## Conclusion

First, it has been shown that small atoms such as lithium and carbon can be encapsulated in $C_{36}$ on the basis of the calculation of their encapsulation energies. Especially, they are expected to be encapsulated in $C_{36}$ more favorably than in $C_{60}$, even though the cavity size of the former is only 70% of that of the latter. This leads us to conjecture that the fullerene could house other small atoms such as beryllium and boron, although it is not clear if it can encase a nitrogen atom. It will be very interesting to verify this prediction experimentally, since $C_{36}$ is the first fullerene smaller than $C_{60}$ which can be produced in macroscopic amounts. Contrary to the case of $N@C_{60}$, the carbon atom is not located at the center of the cage. Rather, the atom is covalently bonded to carbon atoms of the cage. The spin configuration of the endohedral complexes depends on the size of the cage, although there is a striking similarity in the geometrical features of $C@C_{36}$ and $C@C_{60}$ around the encapsulated carbon. $C@C_{60}$ is also interesting in relation to its application to storage devices, since the equilibrium between two kinds of isomers involves spin quenching and generation.

$Li@C_{36}$ and $C@C_{36}$ are expected to exist in the form of dimers ($Li@C_{36}-C_{36}$ and $C@C_{36}-C_{36}$) with a nonendohedral fullerene rather than as monomers. There are three stable isomers (A, B, and C) for $Li@C_{36}-C_{36}$, where only one stable Li site was identified inside the cavity for each of them. Equilibrium between A and C as well as that between B and C is accompanied by spin transfer between two fullerene units, while that between A and B is not. Meanwhile, there are two stable isomers for $C@C_{36}-C_{36}$, one of which not being observed in the dimer $C_{36}-C_{36}$. Twenty-two distinctive sites were found for the encapsulated carbon atom inside the cavity for each isomer. The calculation of energy barriers shows that they are accessible from one another at room temperature, allowing it to be applicable in data storage. Equilibrium between the two isomers is accompanied by spin quenching and generation, also

making it potentially useful for molecular devices such as magnetic switches.[27] I expect that these predictions could stimulate experimental works on the production of endohedral fullerenes of $C_{36}$ as well as on the understanding of their spin and magnetic properties. Further calculation might be done involving the $D_{2d}$ isomer rather than the $D_{6h}$ isomer, considering that the former was known to form a dimer much more favorably than the latter from a theoretical calculation.[28]

**Acknowledgment.** I appreciate Jeonju University for financial support. I also acknowledge support from KISTI (Korea Institute of Science and Technology Information) under the 7th Strategic Supercomputing Applications Support Program. The use of the computing system of the Supercomputing Center is also greatly appreciated.

## References and Notes

(1) (a) Kroto, H. W.; Heath, J. R.; O'Brien, S. C.; Curl, R. F.; Smalley, R. E.; *Nature* **1985**, *318*, 162. (b) Saunders, M.; Cross, R. J.; Jimenez-Vazquez, H. A.; Shimshi, R.; Khong, A. *Science* **1996**, *271*, 1693. (c) Syamala, M. S.; Cross, R. J.; Saunders, M. *J. Am. Chem. Soc.* **2002**, *124*, 6216. (d) Cross, R. J.; Khong, A.; Saunders, M. *J. Org. Chem.* **2003**, *68*, 8281.

(2) (a) Murphy, T. A.; Pawlic, T.; Weidinger, A.; Hohne, M.; Alcala, R.; Spaeth, J.-M. *Phys. Rev. Lett.* **1996**, *77*, 1075. (b) Weidinger, A.; Waiblinger, M.; Pietzak, B.; Murphy, T. A. *Appl. Phys. A* **1998**, *66*, 287. (c) Mauser, H.; Hommes, N, J,. R. van E.; Clark, T.; Hirsch, A.; Pietzak, B.; Weidinger, A.; Dunsch, L. *Angew. Chem., Int. Ed. Engl.* **1997**, *36*, 2835.

(3) (a) Hino, S.; Takahashi, H.; Iwasaki, K.; Matsumoto, K.; Takafumi, M.; Hasegawa, S.; Kikuchi, K.; Achiba, Y. *Phys. Rev. Lett.* **1993**, *71*, 4261. (b) Poirier, D. M.; Knupfer, M.; Weaver, J. H.; Andreoni, W.; Laasonen, K.; Parrinello, M.; Bethune, D. S.; Kikuchi, K.; Achiba, Y. *Phys. Rev. B* **1994**, *49*, 17403. (c) Kressler, B.; Bringer, A.; Cramm, S.; Schlebusch, C.; Eberhardt, W.; Suzuki, S.; Achiba, Y.; Esch, F.; Barnaba, M.; Cocco, D. *Phys. Rev. Lett.* **1997**, *79*, 2289. (d) Kobayashi, K.; Nagase, S. *Chem. Phys. Lett.* **1998**, *282*, 325.

(4) (a) Iezzi, E. B.; Duchamp, J. C.; Harich, K.; Glass, T. E.; Lee, H. M.; Olmstead, M. M.; Balch, A. L.; Dorn, H. C. *J. Am. Chem. Soc.* **2002**, *124*, 524. (b) Cardona, C. M.; Kitaygorodsky, A.; Echegoyen, L. J. *Am. Chem. Soc.* **2005**, *127*, 10448. (c) Alvarez, L.; Pichler, T.; Georgi, P.; Schwieger, T.; Peisert, H.; Dunsch, L.; Hu, Z.; Knupfer; M.; Fink, J.; Bressler, P.; Mast, M.; Golden, M. S. *Phys. Rev. B* **2002**, *66*, 035107.

(5) Smith, B. W.; Luzzi, D. E.; Achiba, Y. *Chem. Phys. Lett.* **2000**, *331*, 137.

(6) (a) Shinohara, H. *Rep. Prog. Phys.* **2000**, *63*, 843. (b) Toth, E.; Bolskar, R. D.; Borel, A.; Gonzalez, G.; Helm, L.; Merbach, A. E.; Sitharaman, B.; Wilson, L. J. *J. Am. Chem. Soc.* **2005**, *127*, 799.

(7) (a) Murphy, T. A.; Pawlik, T.; Weidinger, A.; Hohne, M.; Alcala, R.; Spaeth, J.-M. *Phys. Rev. Lett.* **1996**, *77*, 1075. (b) Knapp, C.; Dinse, K.-P.; Pietzak, B.; Waiblinger, M.; Weidinger. A. *Chem. Phys. Lett.* **1997**, *272*, 433.

(8) Weiden, N.; Goedde, B.; Kass, H.; Dinse, K.-P. *Phys. Rev. Lett.* **2000**, *85*, 1544.

(9) (a) Piskoti, C.; Yarger, J.; Zettl, A. *Nature* **199**8, *393*, 771. (b) Heath, J. R. *Nature* **1998**, *393*, 730.

(10) Grossman, J. C.; Cote, M.; Louie, S, G.; Cohen, M. L. *Chem. Phys. Lett.* **1998**, *284*, 344.

(11) Collins, P. G.; Grossman, J. C.; Cote, M.; Ishigami, M.; Piskoti, C.; Louie, S. G.; Cohen, M. L.; Zettl, A. *Phys. Rev. Lett.* **1999**, *82*, 165.

(12) Grossman, J. C.; Louie, S. G.; Cohen, M. L. *Phys. Rev. B* **1991**, *60*, R6941.

(13) Cote, M.; Grossman, J. C.; Cohen, M. L.; Louie, S. G. *Phys. Rev. Lett.* **1998**, *81*, 697.

(14) Guo, T.; Diener, M. D.; Chai, Y.; Alford, M. J.; Haufler, R. E.; McClure, S. M.; Ohno, T.; Weaver, J. H.; Scuseria, G. E.; Smalley, R. E. *Science* **1992**, *257*, 1661.

(15) Li, J.-Q.; Huang, X.; Wu, L.-M.; Zhang, Y.-F. *Acta Chim. Sin.* **2000**, *58*, 319.

(16) Slanina, Z.; Chow, T. *J. Nanosci. Nanotechnol.* **2003**, *3*, 303.

(17) Gutlich, P.; Hauser, A.; Spiering, H. *Angew. Chem., Int. Ed. Engl.* **1994**, *33*, 2024.

(18) Kahn, O. *Molecular Magenetism*; VCH: New York, 1993.

(19) Kahn, O.; Martinez, C. J. *Science* **1998**, *279*, 44.

(20) (a) Kresse, G.; Hafner, J. *Phys. Rev. B* **1993**, *47*, RC558. (b) Kresse, G.; Furthmuller, J. *Phys. Rev. B* **1996**, *54*, 11169.

(21) Kresse, G.; Joubert, D. *Phys. Rev. B* **1999**, *59*, 1758.

(22) Perdew, J. P.; Burke, K.; Ernzerhof, M. *Phys. Rev. Lett.* **1996**, *77*, 3865.

(23) (a) Kang, H. S. *J. Phys. Chem. A* **2005**, *109*, 478. (b) Kang, H. S. *J. Phys. Chem. A* **2005**, *109*, 1458. (c) Kang, H. S. *J. Phys. Chem. A* **2005**, *109*, 4342. (d) Kang, H. S. *J. Am. Chem. Soc.* **2005**, *127*, 9839. (e) Kang, H. S. *J. Phys. Chem. A* **2005**, *109*, 9292.

(24) Reed, A. E.; Curtiss, L. E.; Weinhold, F. *Chem. Rev.* **1988**, *88*, 899.

(25) Frisch, M. J.; Trucks, G. W.; Schlegel, H. B.; Scuseria, G. E.; Robb, M. A.; Cheeseman, J. R.; Montgomery, J. A., Jr.; Vreven, T.; Kudin, K. N.; Burant, J. C.; Millam, J. M.; Iyengar, S. S.; Tomasi, J.; Barone, V.; Mennucci, B.; Cossi, M.; Scalmani, G.; Rega, N.; Petersson, G. A.; Nakatsuji, H.; Hada, M.; Ehara, M.; Toyota, K.; Fukuda, R.; Hasegawa, J.; Ishida, M.; Nakajima, T.; Honda, Y.; Kitao, O.; Nakai, H.; Klene, M.; Li, X.; Knox, J. E.; Hratchian, H. P.; Cross, J. B.; Adamo, C.; Jaramillo, J.; Gomperts, R.; Stratmann, R. E.; Yazyev, O.; Austin, A. J.; Cammi, R.; Pomelli, C.; Ochterski, J. W.; Ayala, P. Y.; Morokuma, K.; Voth, G. A.; Salvador, P.; Dannenberg, J. J.; Zakrzewski, V. G.; Dapprich, S.; Daniels, A. D.; Strain, M. C.; Farkas, O.; Malick, D. K.; Rabuck, A. D.; Raghavachari, K.; Foresman, J. B.; Ortiz, J. V.; Cui, Q.; Baboul, A. G.; Clifford, S.; Cioslowski, J.; Stefanov, B. B.; Liu, G.; Liashenko, A.; Piskorz, P.; Komaromi, I.; Martin, R. L.; Fox, D. J.; Keith, T.; Al-Laham, M. A.; Peng, C. Y.; Nanayakkara, A.; Challacombe, M.; Gill, P. M. W.; Johnson, B.; Chen, W.; Wong, M. W.; Gonzalez, C.; Pople, J. A. *Gaussian03*, Revision B.05; Gaussian, Inc.: Pittsburgh, PA, 2003.

(26) (a) Reed, A. E.; Weinstock, R. B.; Weinhold, F. *J. Chem. Phys.* **1985**, *83*, 735. (b) Reed, A. E.; Weinhold, F. *Chem. Rev.* **1988**, *88*, 899. (c) Reed, A. E.; Schleyer, P. v. R. *J. Am. Chem. Soc.* **1990**, *112*, 1434.

(27) As an example, see: Sato, O.; Kawakami, T.; Kimura, M.; Hishiya, S.; Kubo, S.; Einaga, Y. *J. Am. Chem. Soc.* **2004**, *126*, 13176.

(28) Chen, Y.-M.; Liu, R.-Z.; Huang, Y.-H. *Acta Chim. Sin.* **2004**, *62*, 53.